Ballistic vs diffusive low-frequency scaling in the XXZ and a locally perturbed XXZ chain

Marlon Brenes,[1] John Goold,[1] and Marcos Rigol[2]

[1] *School of Physics, Trinity College Dublin, College Green, Dublin 2, Ireland*
[2] *Department of Physics, The Pennsylvania State University, University Park, PA 16802, USA*

We study the matrix elements of local operators in the eigenstates of the integrable XXZ chain and of the quantum chaotic model obtained by locally perturbing the XXZ chain with a magnetic impurity. We show that the low-frequency behavior of the variances of the off-diagonal matrix elements can be starkly different depending on the operator. In the integrable model we find that, as the frequency $\omega \to 0$, the variances are either nonvanishing (generic behavior) or vanishing (for a special class of operators). In the quantum chaotic model, on the other hand, we find the variances to be nonvanishing as $\omega \to 0$ and to indicate diffusive dynamics. We highlight which properties of the matrix elements of local operators are different between the integrable and quantum chaotic models independently of the specific operator selected.

Introduction.— The eigenstate thermalization hypothesis (ETH) [1–5] is the paradigm behind our current understanding for why thermalization occurs in generic (quantum chaotic, nonintegrable) isolated quantum systems and, in particular, in pure states. While pure states remain pure under unitary evolution, i.e., they cannot become any of the mixed states defining traditional ensembles in statistical mechanics (so that thermalization cannot occur at the level of the density matrix of the entire system), observables (few-body operators) can exhibit nontrivial dynamics and equilibration. The matrix elements of observables in the eigenstates of the Hamiltonian, along with the initial state, are the ones that determine the dynamics and expectation values after equilibration. For initial states with subextensive energy fluctuations (which are the ones involved in most experimental situations [4, 5]), it turns out that observables that comply with the ETH are guaranteed to thermalize, i.e., after equilibration their expectation values are described by traditional ensembles of statistical mechanics.

Given an observable $\hat{O}$, the ETH can be written as the following ansatz for the matrix elements $O_{nm} = \langle n|\hat{O}|m\rangle$ in the energy eigenbasis ($\hat{H}|m\rangle = E_m|m\rangle$)

$$O_{nm} = O(\bar{E})\delta_{nm} + e^{-S(\bar{E})/2} f_O(\bar{E},\omega) R_{nm}, \qquad (1)$$

where $\bar{E} \coloneqq (E_n + E_m)/2$ and $\omega \coloneqq E_m - E_n$. $S(\bar{E})$ is the thermodynamic entropy at energy $\bar{E}$, R_{nm} is a random variable with zero mean and unit variance, and $O(\bar{E})$ and $f_O(\bar{E},\omega)$ are smooth functions. The first term is the one that ensures that, if the energy fluctuations are subextensive in the initial state, the equilibrated result is described by ensembles of statistical mechanics. The second term, which because of $e^{-S(\bar{E})/2}$ is exponentially small in the system size, is the one that ensures that time fluctuations are small at long times so that equilibration occurs. Many studies have shown that the behavior of the matrix elements of observables in quantum chaotic systems is described by the ETH ansatz, and that as a result, such systems thermalize under unitary dynamics (see Ref. [5] for a review).

Integrable systems, on the other hand, are a class known not to thermalize under unitary dynamics for generic (experimentally relevant) initial states [6–10]. Because of the presence of an extensive number of nontrivial conserved quantities, the structure of the matrix elements of observables in integrable systems is different from the one prescribed by the ETH. Two fundamental differences between the behavior of the diagonal matrix elements of observables in integrable and nonintegrable systems at any given energy are that in integrable systems the eigenstate to eigenstate fluctuations do not vanish in the thermodynamic [4, 7, 11–16] while their variance vanishes as a power law in the system size [15, 17–19], in contrast to the exponential vanishing with system size of the eigenstate to eigenstate fluctuations and their variance in nonintegrable systems [13–15, 20–23]. For the off-diagonal matrix elements of observables, the main difference between interacting integrable systems and quantum chaotic ones is that in the former the matrix elements are close to log-normal distributed [15] while in the latter they are Gaussian distributed [15, 16, 24, 25].

Breaking integrability weakly leads to anomalous unitary dynamics and, specifically, to prethermalization [26–37]. Namely, to dynamics that at short times is dictated by the unperturbed integrable Hamiltonian (fast prethermal dynamics), followed by slow thermalizing dynamics dictated by the perturbation [37]. The strength of a global perturbation needed for quantum chaos and thermalization to occur is expected to vanish in the thermodynamic limit [12, 38–42]. Remarkably, even a local perturbation such as a magnetic impurity added to an integrable spin chain has been shown to lead to quantum chaos and eigenstate thermalization [16, 43–49].

Two recent preprints have explored novel effects of breaking integrability with a local perturbation [16, 42]. In Ref. [16], we showed that the diagonal matrix elements of local operators away from the impurity satisfy the ETH with the smooth $O(\bar{E})$ function in Eq. (1) yielding the microcanonical ensemble predictions for the integrable model, while the off-diagonal matrix elements are Gaussian distributed and comply to with ETH scaling prescribed by Eq. (1). We also showed that, remark-

ably, at low frequency the variance of the off-diagonal matrix elements of the total spin current operator in the perturbed model exhibits the same ballistic scaling as in the unperturbed integrable model. This is consistent with the finding in Ref. [49] that transport is ballistic in the quantum chaotic model. Pandey *et al.* [42], on the other hand, explored how the norm of the so-called adiabatic gauge potential (the AGP norm) can be used to probe the emergence of quantum chaos. The AGP norm depends on the variance of the off-diagonal matrix elements of the operator used as perturbation, as well as the energy level spacing, both in the unperturbed Hamiltonian. A remarkable finding in Ref. [42] is that, depending on the operator chosen to perturb the integrable model, the AGP norm exhibits different scaling with system size. For operators that do not break integrability, the AGP norm scales polynomially, while for operators that break integrability it scales exponentially (as in quantum chaotic models). Hence, the latter operators do not allow one to probe the integrability of the unperturbed model.

One of the goals of this rapid communication is to explore how the low-frequency behavior of the variance of the off-diagonal matrix elements depends on the operator chosen. This will allow us to connect the findings in Refs. [16] and [42], as well as to understand the origin of the difference in scaling of the AGP norm found in Ref. [42]. Another goal of this work is to identify which properties of the matrix elements of local operators are different between the integrable and quantum chaotic model independently of the specific operator selected. Those properties allow one to identify a model as integrable independently of the scaling of the AGP norm.

Hamiltonian and observables.— As in Refs. [16, 42], our unperturbed integrable model is the XXZ chain with Hamiltonian (we set $\hbar = 1$):

$$\hat{H}_{\rm XXZ} = \sum_{i=1}^{N-1} \left(\hat{\sigma}_i^x \hat{\sigma}_{i+1}^x + \hat{\sigma}_i^y \hat{\sigma}_{i+1}^y + \Delta\, \hat{\sigma}_i^z \hat{\sigma}_{i+1}^z \right), \qquad (2)$$

where $\hat{\sigma}_i^\nu$, $\nu = x, y, z$, are the ν-Pauli matrices at site i in a chain with N (even) sites and open boundary conditions. We consider two values of the anisotropy parameter Δ, $\Delta = 0.55$ in the easy-plane regime (as in Ref. [16]) and $\Delta = 1.1$ in the easy-axis regime (as in Ref. [42]). We explore the similarities (differences) in the behavior of the matrix elements of local operators in those regimes.

We perturb the XXZ chain, placing a magnetic impurity at site $N/2$, which is known to result in a Wigner-Dyson distribution of nearest neighbors level spacings [43–49]. The single-impurity Hamiltonian reads

$$\hat{H}_{\rm SI} = \hat{H}_{\rm XXZ} + h\, \hat{\sigma}_{N/2}^z, \qquad (3)$$

where h (set to $h = 1$) is the impurity field strength.

The $\hat{H}_{\rm XXZ}$ and $\hat{H}_{\rm SI}$ Hamiltonians commute with the total magnetization $\hat{S}^z = \sum_i \hat{\sigma}_i^z$, $[\hat{H}_{\rm XXZ}, \hat{S}^z] = [\hat{H}_{\rm SI}, \hat{S}^z] = 0$. Our calculations are carried out within the zero magnetization sector, $\langle \hat{S}^z \rangle = 0$, which is the largest one. In $\hat{H}_{\rm SI}$, reflection symmetry is broken by the impurity. In the calculations involving $\hat{H}_{\rm XXZ}$, we break reflection symmetry by adding a very weak magnetic field at site $i = 1$ ($h_1 = 10^{-1}$). The latter perturbation, like open boundary conditions, does not break integrability [43]. We use full exact diagonalization calculations to compute the matrix elements of observables in the energy eigenbasis. We consider chains with up to $N = 20$ sites, for which the dimension of the Hilbert space of the zero magnetization sector is $\mathcal{D} = N!/[(N/2)!]^2 = 184\,756$.

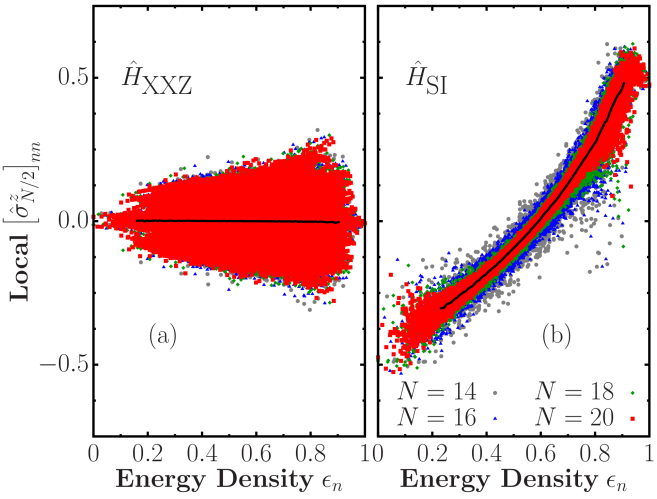

FIG. 1. Diagonal matrix elements of the magnetization at $N/2$, $\hat{\sigma}^z_{N/2}$, in the eigenstates of the (integrable) XXZ (a) and (nonintegrable) single-impurity (b) models, for different chain sizes N and $\Delta = 0.55$. The black lines correspond to the microcanonical averages (within windows with $\delta\epsilon_n = 0.008$) for the largest chain ($N = 20$).

We focus on two local operators, the magnetization at site $N/2$, $\hat{\sigma}^z_{N/2}$, which is the operator used to locally perturb the XXZ chain to break its integrability, and the total "kinetic" energy per site

$$\hat{T} := \frac{1}{N} \sum_{i=1}^{N-1} \left(\hat{\sigma}_i^x \hat{\sigma}_{i+1}^x + \hat{\sigma}_i^y \hat{\sigma}_{i+1}^y \right). \qquad (4)$$

In Ref. [42], it was found that the AGP norm of $\hat{\sigma}^z_{N/2}$ at the integrable point scales with N as the AGP norm of local operators in quantum chaotic systems. This opens the question of whether $\hat{\sigma}^z_{N/2}$ exhibits any ETH like behavior at integrability. $\hat{T}$, on the other hand, does not break integrability if added to the XXZ chain (one gets a new XXZ chain) and its AGP norm at the integrable point scales differently from the AGP norm of $\hat{\sigma}^z_{N/2}$ [42].

Diagonal ETH.— In Fig. 1, we plot the diagonal matrix elements of $\hat{\sigma}^z_{N/2}$ in the eigenstates of $\hat{H}_{\rm XXZ}$ [Fig. 1(a)] and $\hat{H}_{\rm SI}$ [Fig. 1(b)] for $\Delta = 0.55$ (qualitatively similar results were obtained for $\Delta = 1.1$, not shown). We plot the matrix elements vs the energy density ϵ_n defined as $\epsilon_n := E_n - E_{\rm min}/E_{\rm max} - E_{\rm min}$, where E_n is the *nth* energy

eigenvalue, and $E_{\rm min}$ ($E_{\rm max}$) is the ground state (highest) energy eigenvalue. Figure 1(a) shows that there is no diagonal eigenstate thermalization for this observable in the XXZ chain because the support of the eigenstate to eigenstate fluctuations of $[\hat{\sigma}^z_{N/2}]_{nn}$, at any given energy, does not decrease with increasing system size. This is in contrast to the results for the single-impurity model in which the support of the eigenstate to eigenstate fluctuations of $[\hat{\sigma}^z_{N/2}]_{nn}$, at any given energy away from the edges of the spectrum, decreases with increasing system size. This suggests that diagonal eigenstate thermalization occurs for $\hat{\sigma}^z_{N/2}$ in the single-impurity model.

The results for $[\hat{\sigma}^z_{N/2}]_{nn}$ are in qualitative agreement with the results reported for $[\hat{T}]_{nn}$ in Ref. [16], suggesting that diagonal eigenstate thermalization occurs for local operators in the single-impurity model but not in the integrable XXZ chain. A difference to be highlighted between the diagonal ETH for $\hat{T}$ and $\hat{\sigma}^z_{N/2}$ in the single-impurity model is that for $\hat{T}$ the smooth function $T(E)$ is the microcanonical prediction for the integrable model (because $\hat{T}$ is an average over the entire chain and the magnetic impurity is a subextensive perturbation [16]) while this is clearly not the case for the smooth function $\sigma^z_{N/2}(E)$ of $\hat{\sigma}^z_{N/2}$ in Fig. 1(b). The latter is expected given that $\hat{\sigma}^z_{N/2}$ is the operator used to perturb the XXZ chain.

Off-diagonal ETH.— Next we study the off-diagonal matrix elements of $\hat{\sigma}^z_{N/2}$. We explore whether they share properties in the XXZ chain with those of the matrix elements of local operators in quantum chaotic systems.

In Fig. 2, we plot the average $\overline{|[\hat{\sigma}^z_{N/2}]_{nm}|^2}$ vs ω in the eigenstates of $\hat{H}_{\rm XXZ}$ [Fig. 2(a)] and $\hat{H}_{\rm SI}$ [Fig. 2(b)] for $\Delta = 0.55$ (qualitatively similar results were obtained for $\Delta = 1.1$, not shown). Since $\overline{[\hat{\sigma}^z_{N/2}]_{nm}} = 0$, those averages are the variances of the off-diagonal matrix elements. One can see in Fig. 2 that the results for the variances of the off-diagonal matrix elements of $\hat{\sigma}^z_{N/2}$ are qualitatively (and even quantitatively) similar for the integrable [Fig. 2(a)] and quantum chaotic [Fig. 2(b)] models. For both models, we find the variances to be smooth functions of ω that decay rapidly at high ω (the specific scaling with ω, at high ω, are discussed in Ref. [15]). In Fig. 2, we report results for four chain sizes. They exhibit a near perfect collapse in Fig. 2(b) showing that, in the quantum chaotic model, the variances scale as $1/\mathcal{D}$ as expected from the ETH in the "infinite-temperature" regime, namely, when $\bar{E} \approx 0$ and $S(\bar{E}) \approx \ln \mathcal{D}$. The same collapse is seen in Fig. 2(a) and shows that, as found in Ref. [15], the variances exhibit the same scaling in the interacting integrable XXZ model.

The results in Fig. 2 for the variance of the off-diagonal matrix elements of $\hat{\sigma}^z_{N/2}$ in the XXZ and single-impurity models are qualitatively similar to the ones reported in Ref. [16] for $\hat{T}$. Put together these results show that, within the frequency scales in Fig. 2 there are no qualitative differences between the integrable and quantum chaotic models neither for the same nor for different local

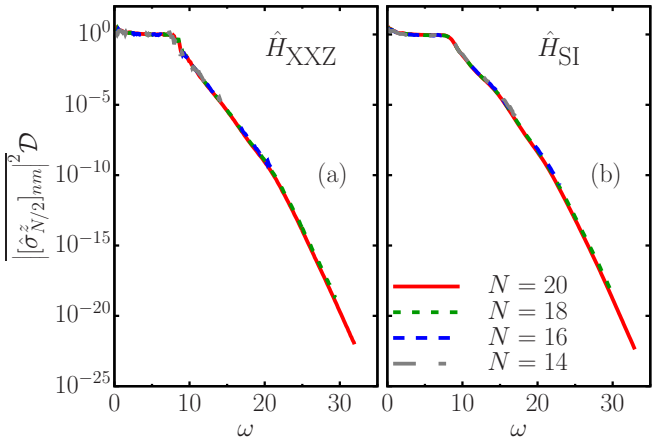

FIG. 2. Average $\overline{|[\hat{\sigma}^z_{N/2}]_{nm}|^2}$ vs ω in the XXZ (a) and single-impurity (b) models, for different chain sizes N and $\Delta = 0.55$. The matrix elements are computed from pairs of states whose $\bar{E}$ lie within the interval $[\bar{E} - 0.05\varepsilon/2, \bar{E} + 0.05\varepsilon/2]$, where $\varepsilon := E_{\rm max} - E_{\rm min}$ denotes the bandwidth. The averages in ω were carried out in windows $\delta\omega = 0.1$.

operators. To reveal the existence of qualitative differences between the off-diagonal matrix elements of local operators in integrable and quantum chaotic systems, at the frequency scales in Fig. 2, one needs to study their distributions. The off-diagonal matrix elements of local operators in quantum chaotic systems have been found to be normally distributed [15, 16, 24, 25], while they have been found to be close to log-normally distributed in the translationally invariant integrable XXZ chain [15].

To test whether the off-diagonal matrix elements of $\hat{\sigma}^z_{N/2}$ are normally distributed in any of the two models considered here, for different values of ω, we compute [15]

$$\Gamma_{\hat{\sigma}^z_{N/2}}(\omega) := \overline{|[\hat{\sigma}^z_{N/2}]_{nm}|^2} / \overline{|[\hat{\sigma}^z_{N/2}]_{nm}|}^2 . \qquad (5)$$

$\Gamma_{\hat{\sigma}^z_{N/2}} = \pi/2$ for normally distributed matrix elements.

In Fig. 3, we plot $\Gamma_{\hat{\sigma}^z_{N/2}}$ vs ω in the eigenstates of $\hat{H}_{\rm XXZ}$ [Fig. 3(a)] and $\hat{H}_{\rm SI}$ [Fig. 3(b)] for $\Delta = 0.55$ (qualitatively similar results were obtained for $\Delta = 1.1$, not shown). For the quantum chaotic model [Fig. 3(b)], we find that the window in ω for which $\Gamma_{\hat{\sigma}^z_{N/2}}$ is essentially $\pi/2$ increases with increasing system size. We conclude from these results that, for sufficiently large system sizes, the off-diagonal matrix elements of $\hat{\sigma}^z_{N/2}$ in the single-impurity model are normally distributed independently of the value of ω (the expectation for an ETH satisfying system). On the other hand, for the integrable XXZ chain [Fig. 3(a)], the results for $\Gamma_{\hat{\sigma}^z_{N/2}}$ fail to collapse for different systems sizes showing that the off-diagonal matrix elements of $\hat{\sigma}^z_{N/2}$ are not normally distributed. Since the AGP norm for $\hat{\sigma}^z_{N/2}$ in the XXZ chain scales as in quantum chaotic models [42], the distribution of off-diagonal matrix elements of $\hat{\sigma}^z_{N/2}$ can be used to identify this model as integrable. We should add that the results

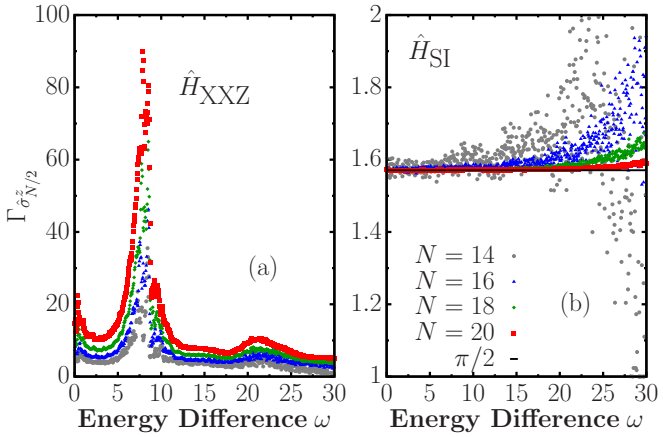

FIG. 3. $\Gamma_{\hat{\sigma}^z_{N/2}}$ vs ω, see Eq. (5), in the XXZ (a) and single-impurity (b) models, for different chain sizes N and $\Delta = 0.55$. The horizontal line in (b) marks $\pi/2$. The matrix elements were computed using the same energy window as in Fig. 2, while the coarse-graining parameter was chosen to be $\delta\omega = 0.05$.

in Fig. 3 for $\Gamma_{\hat{\sigma}^z_{N/2}}$ are qualitatively similar to the ones reported in Ref. [16] for $\Gamma_{\hat{T}}$.

Variances at low frequency.— Next, we study the low-frequency behavior of the variances of $\hat{\sigma}^z_{N/2}$ (which are behind the "ETH-like" scaling of the AGP norm in the XXZ chain [42]) and of $\hat{T}$ (which are behind the "integrable-like" scaling of the AGP norm in the XXZ chain [42]). One of our goals is to identify the distinguishing signatures of integrability and quantum chaos.

In Figs. 4(a) and 4(c), we show the scaled variances of the off-diagonal matrix elements of $\hat{\sigma}^z_{N/2}$ and $\hat{T}$, respectively, in the XXZ chain for $\Delta = 0.55$ (main panels) and $\Delta = 1.1$ (insets). The extra N factor in the y-axis in Fig. 4(c) accounts for the Hilbert-Schmidt norm of $\hat{T}$ [16]. For both observables and both values of Δ, we find a regime in ω in which the variances indicate ballistic dynamics (they are functions of $N\omega$, see the curves collapse for different system sizes at intermediate values of $N\omega$) [5]. The collapse degrades as $N\omega$ decreases. This can either be a signature of diffusive dynamics at longer times or just a result of finite-size effects. Further works will need to clarify this. For $\omega \to 0$, Figs. 4(a) and 4(c) show that the variances of $\hat{\sigma}^z_{N/2}$ and $\hat{T}$, respectively, are starkly different. While for both values of Δ they are nonvanishing in Fig. 4(a), they vanish in Fig. 4(c).

Figures 4(b) and 4(d), on the other hand, show the remarkable effect that the single-impurity integrability breaking perturbation has on the low-frequency behavior of the variances. For both observables and both values of Δ, the variances become clearly nonvanishing as $\omega \to 0$, and they exhibit a plateau for small values of $N^2\omega$ indicating diffusive dynamics (finite-size effects appear to affect more the magnitude of the variances of $\hat{T}$ than of $\hat{\sigma}^z_{N/2}$) as expected of quantum chaotic systems [5].

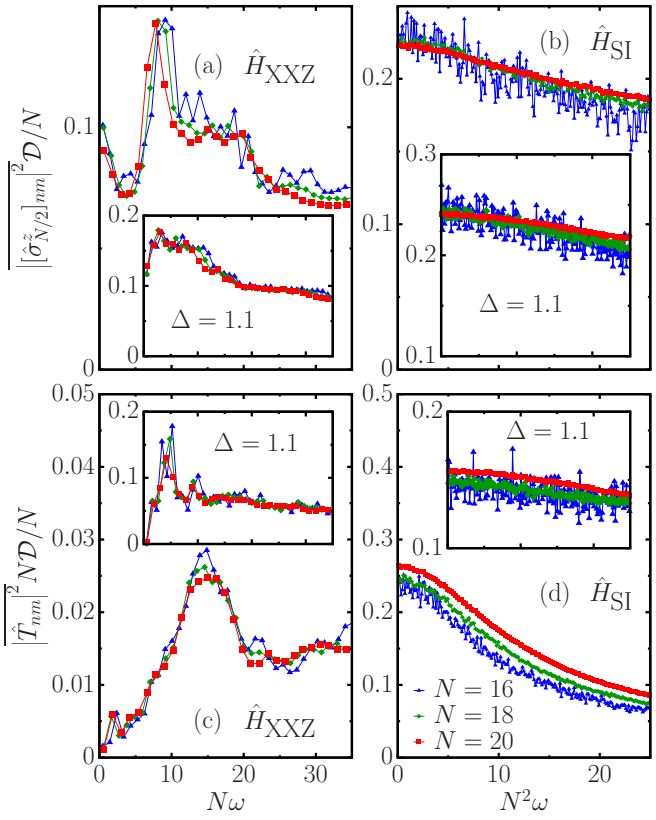

FIG. 4. Scaled variances of the off-diagonal matrix elements of $\hat{\sigma}^z_{N/2}$ [(a),(b)] and $\hat{T}$ [(c),(d)] in the XXZ [(a),(c)] and single-impurity [(b),(d)] models, for different chain sizes N. The main panels show results for $\Delta = 0.55$ while the insets show results for $\Delta = 1.1$. The matrix elements were computed within a small window of energies around $\bar{E} \approx 0$ of width 0.075ε. For the binned averages, we used $\delta\omega = 0.06$ for the integrable [(a),(c)] and $\delta\omega = 5\times10^{-4}$ for the quantum chaotic [(a),(c)] models, such that smooth curves are obtained that are robust against small changes in $\delta\omega$.

Summary and discussion.— We have shown that the diagonal, and the distribution of the off-diagonal, matrix elements of local operators exhibit distinctive behavior in integrable and quantum chaotic models independently of the operator chosen. The variances of the off-diagonal matrix elements at intermediate and high frequencies, on the other hand, do not allow one to distinguish integrable from quantum chaotic models. Instead, one needs to study the low-frequency behavior of the variances to observe differences. For $\omega \to 0$, we found the variances to be nonvanishing in the quantum chaotic model and for the operator that breaks integrability in the integrable one ($\hat{\sigma}^z_{N/2}$), while they vanish for the operator that does not break integrability in the integrable model ($\hat{T}$).

The $\omega \to 0$ behavior of the variances observed for $\hat{\sigma}^z_{N/2}$ and $\hat{T}$ at integrability explain the difference in scaling of their AGP norm observed in Ref. [42]. Since generic operators are expected to break integrability if added as perturbations to an interacting integrable model, we ex-

pect the low-frequency behavior identified here for the variance of the off-diagonal matrix elements of $\hat{\sigma}^z_{N/2}$ to be generic in integrable models (we have already checked that for several observables). This means that using generic operators to compute the AGP norm at integrability does not allow one to identify the model as integrable, because the AGP norm would scale as it does for local operators in quantum chaotic systems. Our results in Fig. 3 show that, in such situations, studying the distribution of the off-diagonal matrix elements of the operator allows one to distinguish between the two.

In the quantum chaotic model generated by the single impurity perturbation of the XXZ chain, we found that at low-frequencies the variances of local operators indicate diffusive dynamics (as expected for generic quantum chaotic systems [5]). That said, in Ref. [16] we showed that the variance of the off-diagonal matrix elements of the total spin current operator in the perturbed model exhibits the same ballistic scaling as in the unperturbed integrable model (consistent with the ballistic nature of spin transport in both models [49]). All other properties of the matrix elements of the current operator complied with the ETH in the perturbed model but not in the unperturbed integrable one. Whether a low-frequency diffusive plateau emerges in larger systems sizes for the current operator is an open question. Further open questions include whether there are similar exceptions of lack of low-frequency diffusive scaling in other quantum chaotic models (even if only in similar-sized systems), and, if they do, for which classes of operators they occur.

Acknowledgements.— We are grateful to T. LeBlond, A. Polkovnikov, and L. Vidmar for insightful discussions. This work was supported by the European Research Council Starting Grant ODYSSEY Grant No. 758403 (M.B. and J.G.), the Royal Society (M.B.), a SFI-Royal Society University Research Fellowship (J.G.), and the National Science Foundation Grant No. PHY-1707482 (M.R.). M.B. and J.G. acknowledge the DJEI/DES/SFI/HEA Irish Centre for High-End Computing (ICHEC) for the provision of computational facilities and support, project TCPHY118B, and the Trinity Centre for High-Performance Computing.

[1] J. M. Deutsch, Phys. Rev. A **43**, 2046 (1991).
[2] M. Srednicki, Phys. Rev. E **50**, 888 (1994).
[3] M. Srednicki, J. Phys. A **32**, 1163 (1999).
[4] M. Rigol, V. Dunjko, and M. Olshanii, Nature **452**, 854 (2008).
[5] L. D'Alessio, Y. Kafri, A. Polkovnikov, and M. Rigol, Adv. Phys. **65**, 239 (2016).
[6] M. Rigol, V. Dunjko, V. Yurovsky, and M. Olshanii, Phys. Rev. Lett. **98**, 050405 (2007).
[7] L. Vidmar and M. Rigol, J. Stat. Mech. **2016**, 064007 (2016).
[8] F. H. L. Essler and M. Fagotti, J. Stat. Mech. **2016**, 064002 (2016).
[9] J.-S. Caux, J. Stat. Mech. **2016**, 064006 (2016).
[10] M. Rigol, Phys. Rev. Lett. **116**, 100601 (2016).
[11] M. Rigol, Phys. Rev. Lett. **103**, 100403 (2009); Phys. Rev. A **80**, 053607 (2009).
[12] L. F. Santos and M. Rigol, Phys. Rev. E **82**, 031130 (2010).
[13] R. Steinigeweg, J. Herbrych, and P. Prelovšek, Phys. Rev. E **87**, 012118 (2013).
[14] W. Beugeling, R. Moessner, and M. Haque, Phys. Rev. E **89**, 042112 (2014).
[15] T. LeBlond, K. Mallayya, L. Vidmar, and M. Rigol, Phys. Rev. E **100**, 062134 (2019).
[16] M. Brenes, T. LeBlond, J. Goold, and M. Rigol, arXiv:2004.04755.
[17] G. Biroli, C. Kollath, and A. M. Läuchli, Phys. Rev. Lett. **105**, 250401 (2010).
[18] T. N. Ikeda, Y. Watanabe, and M. Ueda, Phys. Rev. E **87**, 012125 (2013).
[19] V. Alba, Phys. Rev. B **91**, 155123 (2015).
[20] H. Kim, T. N. Ikeda, and D. A. Huse, Phys. Rev. E **90**, 052105 (2014).
[21] R. Mondaini, K. R. Fratus, M. Srednicki, and M. Rigol, Phys. Rev. E **93**, 032104 (2016).
[22] T. Yoshizawa, E. Iyoda, and T. Sagawa, Phys. Rev. Lett. **120**, 200604 (2018).
[23] D. Jansen, J. Stolpp, L. Vidmar, and F. Heidrich-Meisner, Phys. Rev. B **99**, 155130 (2019).
[24] W. Beugeling, R. Moessner, and M. Haque, Phys. Rev. E **91**, 012144 (2015).
[25] R. Mondaini and M. Rigol, Phys. Rev. E **96**, 012157 (2017).
[26] M. Moeckel and S. Kehrein, Phys. Rev. Lett. **100**, 175702 (2008); Ann. Phys. **324**, 2146 (2009).
[27] M. Eckstein, M. Kollar, and P. Werner, Phys. Rev. Lett. **103**, 056403 (2009).
[28] M. Kollar, F. A. Wolf, and M. Eckstein, Phys. Rev. B **84**, 054304 (2011).
[29] M. Tavora and A. Mitra, Phys. Rev. B **88**, 115144 (2013).
[30] M. Tavora, A. Rosch, and A. Mitra, Phys. Rev. Lett. **113**, 010601 (2014).
[31] N. Nessi, A. Iucci, and M. A. Cazalilla, Phys. Rev. Lett. **113**, 210402 (2014).
[32] F. H. L. Essler, S. Kehrein, S. R. Manmana, and N. J. Robinson, Phys. Rev. B **89**, 165104 (2014).
[33] B. Bertini, F. H. L. Essler, S. Groha, and N. J. Robinson, Phys. Rev. Lett. **115**, 180601 (2015); Phys. Rev. B **94**, 245117 (2016).
[34] M. Fagotti and M. Collura, arXiv:1507.02678.
[35] F. Lange, Z. Lenarčič, and A. Rosch, Phys. Rev. B **97**, 165138 (2018).
[36] P. Reimann and L. Dabelow, Phys. Rev. Lett. **122**, 080603 (2019).
[37] K. Mallayya, M. Rigol, and W. De Roeck, Phys. Rev. X **9**, 021027 (2019).
[38] D. A. Rabson, B. N. Narozhny, and A. J. Millis, Phys. Rev. B **69**, 054403 (2004).
[39] L. F. Santos and M. Rigol, Phys. Rev. E **81**, 036206 (2010).
[40] R. Modak, S. Mukerjee, and S. Ramaswamy, Phys. Rev.

B **90**, 075152 (2014).
[41] R. Modak and S. Mukerjee, New J. Phys. **16**, 093016 (2014).
[42] M. Pandey, P. W. Claeys, D. K. Campbell, A. Polkovnikov, and D. Sels, arXiv:2004.05043.
[43] L. Santos, J. Phys. A **37**, 4723 (2004).
[44] L. F. Santos and A. Mitra, Phys. Rev. E **84**, 016206 (2011).
[45] E. Torres-Herrera and L. F. Santos, Phys. Rev. E **89**, 062110 (2014).
[46] E. J. Torres-Herrera, D. Kollmar, and L. F. Santos, Phys. Scr. **T165**, 014018 (2015).
[47] O. S. Barišić, P. Prelovšek, A. Metavitsiadis, and X. Zotos, Phys. Rev. B **80**, 125118 (2009).
[48] A. Metavitsiadis, X. Zotos, O. S. Barišić, and P. Prelovšek, Phys. Rev. B **81**, 205101 (2010).
[49] M. Brenes, E. Mascarenhas, M. Rigol, and J. Goold, Phys. Rev. B **98**, 235128 (2018).